Interaction of the Human Adenovirus Proteinase with Its 11-Amino Acid Cofactor pVIc†

Mary Lynn Baniecki,‡ William J. McGrath,§ Sarah M. McWhirter,§ Caroline Li,§ Diana L. Toledo,§ Patricia Pellicena,|| Dale L. Barnard,⊥ Kurt S. Thorn,# and Walter F. Mangel*,§

Department of Pharmacological Sciences, State University of New York at Stony Brook, Stony Brook, New York 11794, Biology Department, Brookhaven National Laboratory, Upton, New York 11973, Department of Physiology and Biophysics, State University of New York at Stony Brook, Stony Brook, New York 11794, Institute for Antiviral Research, Utah State University, Logan, Utah 84322-5600, and Graduate Group in Biophysics, University of California at San Francisco, San Francisco, California 94143

Received May 2, 2001; Revised Manuscript Received July 17, 2001

ABSTRACT: The interaction of the human adenovirus proteinase (AVP) and AVP−DNA complexes with the 11-amino acid cofactor pVIc was characterized. The equilibrium dissociation constant for the binding of pVIc to AVP was 4.4 μM. The binding of AVP to 12-mer single-stranded DNA decreased the K_d for the binding of pVIc to AVP to 0.09 μM. The pVIc−AVP complex hydrolyzed the substrate with a Michaelis constant (K_m) of 3.7 μM and a catalytic rate constant (k_{cat}) of 1.1 s^{-1}. In the presence of DNA, the K_m increased less than 2-fold, and the k_{cat} increased 3-fold. Alanine-scanning mutagenesis was performed to determine the contribution of individual pVIc side chains in the binding and stimulation of AVP. Two amino acid residues, Gly1′ and Phe11′, were the major determinants in the binding of pVIc to AVP, while Val2′ and Phe11′ were the major determinants in stimulating enzyme activity. Binding of AVP to DNA greatly suppressed the effects of the alanine substitutions on the binding of mutant pVIcs to AVP. Binding of either or both of the cofactors, pVIc or the viral DNA, to AVP did not dramatically alter its secondary structure as determined by vacuum ultraviolet circular dichroism. pVIc, when added to Hep-2 cells infected with adenovirus serotype 5, inhibited the synthesis of infectious virus, presumably by prematurely activating the proteinase so that it cleaved virion precursor proteins before virion assembly, thereby aborting the infection.

Like many virus-coded proteinases, the human adenovirus serotype 2 proteinase (AVP)[1] is required for the synthesis of infectious virus (*1*). Late in infection, young virions are formed in which six of the 12 different major proteins are present in precursor form. In the young virion, approximately 70 AVP molecules become activated (*2*), and they cleave multiple copies of the six virion precursor proteins more than 3200 times, thereby rendering the virus particle infectious (*3*). A temperature-sensitive mutant of adenovirus was shown to lack proteinase activity at the nonpermissive temperature (*1*); the mutation mapped to the L3 23K gene (*4*). The L3 23K gene has been cloned and expressed in *Escherichia coli*, and the resultant 204-amino acid protein, AVP, has been purified (*5*−*7*).

An unusual aspect of AVP is that it requires two cofactors for maximal activity. One cofactor is pVIc, the 11-amino acid peptide from the C-terminus of the precursor to protein VI, pVI. The amino acid sequence of pVIc is GVQSLKRRRCF (*5*, *8*). The four amino acid residues preceding pVIc in pVI constitute an AVP consensus cleavage sequence; thus, AVP can cleave out its own cofactor. Another cofactor is adenovirus DNA (Ad DNA) to which AVP binds nonspecifically, i.e., independent of any specific DNA sequence (*5*). The two cofactors increase the specificity constant, k_{cat}/K_m, for substrate hydrolysis. For an AVP−pVIc complex, the level of increase in k_{cat}/K_m, relative to AVP alone, is 1130; for an AVP−Ad DNA complex, it is 110, and for an AVP−pVIc−Ad DNA complex, it is 34100 (*31*).

† Research by W.F.M. supported by the Office of Biological and Environmental Research of the U.S. Department of Energy under Prime Contract DE-AC0298CH10886 with Brookhaven National Laboratory, and by National Institutes of Health Grant AI41599. D.L.B. was supported by Grant RO1-AI35178. S.M.M. and C.L. were supported by the U.S. Department of Energy's Office of Science Education and Technical Information, as Science and Engineering Research Semester Program participants. K.S.T. is supported by a Howard Hughes Medical Institute Predoctoral Fellowship. The National Synchrotron Light Source is supported by the Division of Chemical Sciences and the Division of Materials Sciences, Office of Basic Energy Sciences, U.S. Department of Energy.

* To whom correspondence should be addressed. Telephone: (631) 344-3373. E-mail: mangel@bnl.gov. Fax: (631) 344-3407.

‡ Department of Pharmacological Sciences, State University of New York at Stony Brook.

§ Brookhaven National Laboratory.

|| Department of Physiology and Biophysics, State University of New York at Stony Brook.

⊥ Utah State University.

University of California at San Francisco.

[1] Abbreviations: AVP, adenovirus proteinase 2; CD, circular dichroism; CPE, cytopathic effect; DMF, dimethylformamide; DMSO, dimethyl sulfoxide; DTNB or Ellman's reagent, 5,5′-dithiobis(2-nitrobenzoate); DTT, dithiothreitol; FBS, fetal bovine serum; HMPMA, (*S*)-9-(3-hydroxy-2-phosphonylmethoxypropyl)adenine; k_{cat}, catalytic rate constant for substrate hydrolysis; K_d, equilibrium dissociation constant; K_m, Michaelis constant; MEM, minimal essential medium; pVIc, 11-amino acid peptide, GVQSLKRRRCF, that originates from the C-terminus of the viral precursor protein pVI.

10.1021/bi0109008 CCC: $20.00
Published on Web 09/22/2001

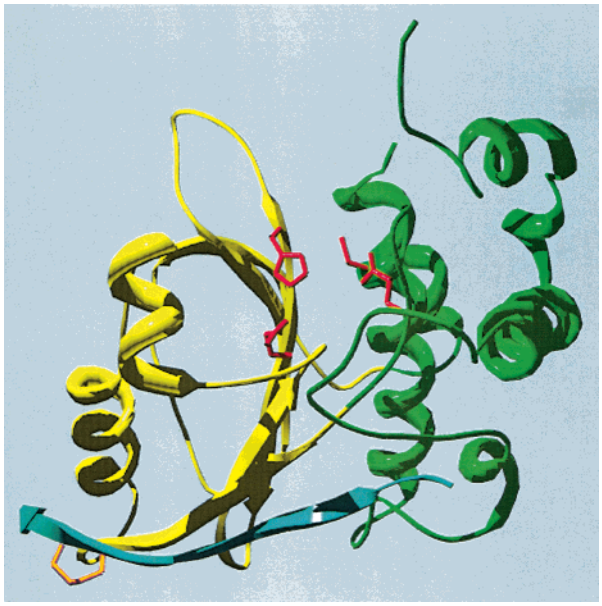

FIGURE 1: Structure of the AVP−pVIc complex. The two domains of AVP are colored yellow and green. pVIc is colored cyan. The residues involved in catalysis in the active site are colored red. The disulfide bond between Cys104 of AVP and Cys10′ of pVIc is colored orange.

Our model for the temporal and spatial regulation of AVP activity illustrates how the virus could make use of the cofactors. AVP is initially synthesized in an inactive form and remains inactive until it enters virions which are in part assembled from precursor proteins. If the proteinase were active before virion assembly, it would prematurely cleave virion precursor proteins. Presumably, cleaved precursor proteins cannot form virus particles. Late in infection, in the nucleus, virion proteins assemble into empty capsids (*10*). Once formed, the viral DNA and core proteins are encapsidated, generating young virions. We postulate that the proteinase enters the empty capsids along with the viral DNA to which it is bound. The AVP−DNA complexes become positioned next to the proteinase consensus cleavage sites on pVI where cleavage liberates pVIc. Liberated pVIc molecules can then bind to the proteinases that cut them out. The ternary complex, AVP−pVIc−DNA, contains a fully active enzyme capable of cleaving viral precursor proteins. AVP−pVIc complexes encounter and cleave viral precursor proteins by moving along the viral DNA via one-dimensional diffusion, much like RNA polymerase moves along DNA looking for a promoter.

The crystal structure of an AVP−pVIc complex has been determined to 2.6 Å resolution (*11*). The AVP−pVIc complex is ovoid (Figure 1). There are two domains in the protein. One domain contains the large β-sheet and two peripheral α-helices. The other domain is composed mostly of α-helices, one from the N-terminus and the remainder from the C-terminus of AVP. These helices form the lower middle to the wide end of the molecule. pVIc appears to act like a strap that holds the two domains together in a configuration that is optimal for efficient catalysis. The crystal structure of the AVP−pVIc complex indicates it is a cysteine proteinase.

Here, the binding of pVIc to AVP is characterized by measuring the equilibrium dissociation constant, K_d, in the presence and absence of DNA. For AVP−pVIc complexes, the Michaelis constant (K_m) and the catalytic rate constant (k_{cat}) for substrate hydrolysis were determined. To identify amino acid residues in pVIc that are essential for the binding of pVIc to AVP and for the stimulation of AVP activity by pVIc, alanine-scanning mutagenesis was performed. Each amino acid of pVIc, except for Cys10′, was individually replaced with an alanine residue. Characterization of Cys10′ of pVIc will be the subject of a separate communication. The 10 mutant pVIcs were assayed for their ability to bind to AVP in the presence and absence of 12-mer single-stranded (ss) DNA, and the K_d values were determined. With the mutant pVIcs bound to AVP, the K_m and k_{cat} for substrate hydrolysis were measured. Changes in proteinase secondary structure on binding pVIc and DNA were investigated by vacuum circular dichroism. Finally, pVIc was shown to act as an antiviral agent when prematurely introduced to AVP early in an infection.

MATERIALS AND METHODS

Materials. pVIc and the mutants of pVIc were purchased from Research Genetics (Huntsville, AL). The 12-mer ssDNA with the sequence GACGACTAGGAT was purchased from Life Technologies (Rockville, MD). Bovine serum albumin and Ellman's reagent or 5,5′-dithiobis(2-nitrobenzoate) (DTNB) were purchased from Sigma Chemical Co. (St. Louis, MO). Reduce-Imm Column and buffers were purchased from Pierce Chemical Co. (Rockford, IL). Octyl glucoside was purchased from Boehringer Mannheim (Ridgefield, CT). (*S*)-9-(3-Hydroxy-2-phosphonylmethoxypropyl)adenine (HMPMA) was kindly provided by A. Holy (Institute of Organic Chemistry and Biochemistry, Prague, Czech Republic). The fluorogenic substrate (Leu-Arg-Gly-Gly-NH)$_2$−Rhodamine was synthesized and purified as described previously (*5, 12*). AVP was purified as described previously (*5, 13*).

Assay for Proteinase Activity. Assays contained, in 1 mL, 10 mM Tris-HCl (pH 8), 5 mM octyl glucoside, 25 μL of Pierce peptide Reduce-Imm column buffer, 20 nM AVP, and 20 mM NaCl in the absence of DNA or 10 nM AVP and no NaCl in the presence of 1 μM 12-mer ssDNA, 3 μM (Leu-Arg-Gly-Gly-NH)$_2$-rhodamine, and the indicated concentrations of pVIc. Assay mixtures were preincubated for 5 min at 37 °C prior to the addition of substrate to allow the binding equilibrium to be reached. The increase in fluorescence was monitored as a function of time in an ISS (Urbana, IL) PC-1 spectrofluorometer. The excitation wavelength was 492 nm and the emission wavelength 523 nm, both set with a band-pass of 8 nm.

Activity assays for measuring K_d values for the binding of pVIc and mutants of pVIc to AVP or the AVP−DNA complex contained substrate concentrations 5-fold greater than the K_m. Activity assays for measuring K_d values for the binding of pVIc and mutants of pVIc to AVP in the presence of DNA contained concentrations of DNA 5 times greater than the K_d for the binding of AVP to DNA. Activity assays for measuring K_m and k_{cat} for AVP or the AVP−DNA complex saturated with wild-type or mutant pVIc contained concentrations of pVIcs 5-fold greater than their K_d.

Protein Concentrations. Protein concentrations were determined using the BCA protein assay from Pierce Chemical Co. For the concentration of AVP, a calculated molar absorbance coefficient at 280 nm of 26 510 M^{-1} cm^{-1} was

also used (*14*). Prior to an assay, pVIc and the alanine mutants of pVIc were reduced by being passed through the Reduce-Imm column following the manufacturer's instructions. The concentrations of pVIc in the column fractions were determined by titration of the cysteine residues with Ellman's reagent. The titration was performed by incubating 490 μL of Reduce-Imm column buffer, 16.5 μL of Ellman's reagent, and 10 μL of the column fraction. After 10 min at ambient temperature, the absorbance at 412 nm was determined. The concentration of pVIc was calculated using an extinction coefficient for thionitrobenzoate of 14 150 M^{-1} cm^{-1} (*15*).

Concentrations of Assay Components. For those assays in which K_m and k_{cat} were determined, the concentration of wild-type or mutant pVIc was usually 5-fold greater than its K_d for binding to AVP. However, for those mutant pVIcs that had very high K_d values, the concentrations of pVIc were less than saturating. The concentration of the active complex (AVP−pVIc) under those conditions was calculated as follows:

$$[\text{AVP}-\text{pVIc}] = [\text{pVIc}]_0[\text{AVP}]_0/(K_d + [\text{pVIc}]_0)$$

where $[\text{pVIc}]_0$ is the initial concentration of pVIc and $[\text{AVP}]_0$ is the initial concentration of AVP.

Measuring the K_d. The equilibrium dissociation constant, K_d, for the binding of pVIc to AVP was determined as follows. Different concentrations of pVIc, $[\text{pVIc}]_i$, were added to a constant amount of AVP, $[\text{AVP}]_0$. After 5 min at 37 °C, the substrate was added and the rate of substrate hydrolysis, F_i, measured. A plot of F_i versus $[\text{pVIc}]_i$ yields a rectangular hyperbola. From this graph, the concentration of pVIc bound, $[\text{pVIc}]_b$, can be obtained:

$$[\text{pVIc}]_b = [\text{AVP}]_0(F_i/F_{max})$$

where F_{max} is the maximal rate of substrate hydrolysis, i.e., the rate when AVP is saturated with pVIc. The concentration of pVIc free, $[\text{pVIc}]_f$, is

$$[\text{pVIc}]_f = [\text{pVIc}]_i - [\text{pVIc}]_b$$

From a plot of $[\text{pVIc}]_b$ versus $[\text{pVIc}]_f$, the K_d can be calculated.

Calculation of Free Energies. The change in the change in free energy ($\Delta\Delta G_B$) upon binding of an alanine mutant of pVIc to AVP was calculated as follows:

$$\Delta\Delta G_B = -RT \ln[K_{d(\text{mutant})}/K_{d(\text{wild-type})}]$$

where R is the gas constant and T is the absolute temperature.

The change in the change in transition state stabilization ($\Delta\Delta G_T^*$) with an alanine mutant of pVIc bound to AVP was calculated:

$$\Delta\Delta G_T^* = -RT \ln(K_m/k_{cat})_{\text{mutant}} - RT \ln(K_m/k_{cat})_{\text{wild-type}}$$

where k_{cat} is the turnover number and K_m is the Michaelis constant for mutant or wild-type pVIc bound to AVP. $\Delta\Delta G_T^*$ represents the change in free energy to reach the transition state complex (E·S*) from the free enzyme and substrate (E + S).

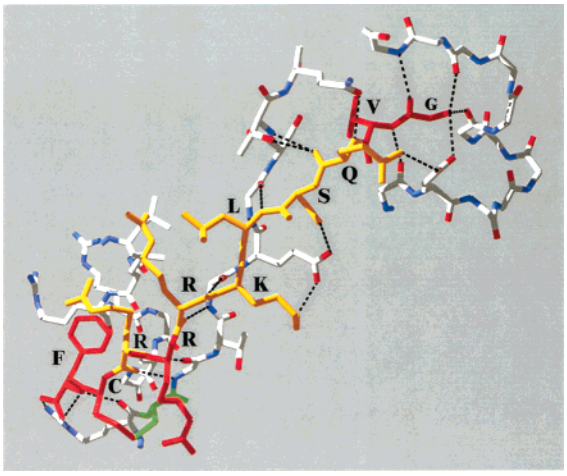

FIGURE 2: Structure of pVIc bound to AVP. The five most conserved amino acids in pVIc (G1′, V2′, R8′, C10′, and F11′) are colored red. The other amino acids in pVI are colored yellow. Hydrogen bonds are depicted as dashed black lines, and Cys104 of AVP is colored green. For AVP, carbon atoms are colored white, nitrogen atoms blue, and oxygen atoms red.

Calculation of Solvent Accessible Surface Areas. Solvent accessible surface areas were calculated using Naccess 2.1.1 (*16*) and are expressed as the percentage of accessible surface area as compared to that of an X-Ala-X tripeptide.

Vacuum Ultraviolet Circular Dichroism. Vacuum ultraviolet circular dichroism (CD) spectra were obtained using the vacuum spectrometer at station U9B of the National Synchrotron Light Source at Brookhaven National Laboratory (*17, 18*). Experiments were performed at room temperature in a quartz cell with a 12.5 μm path length. Protein concentrations were ~5 mg/mL. The value for a background that contained all the components except AVP was subtracted from the experimental data.

Propagation of Cells and Virus. Hep-2 cells, a continuous cell line derived from a human epidermoid carcinoma of the larynx, were obtained from American Type Culture Collection (Rockville, MD). The cells were grown in minimal essential medium (MEM) from Gibco-BRL (Gaithersburg, MD) supplemented with 5% fetal bovine serum (FBS) from Hyclone Laboratories (Logan, UT) and 0.1% $NaHCO_3$. Adenovirus serotype 5 was obtained from American Type Culture Collection.

RESULTS AND DISCUSSION

Interaction between pVIc and AVP Based upon the Crystal Structure. The interaction between pVIc and AVP is extensive and includes main chain hydrogen bonds accompanied by side chain hydrogen bonds, ion pair interactions, van der Waals interactions, and a disulfide bond (Figure 2). There are 24 non-β-strand hydrogen bonds, six β-strand hydrogen bonds, and one covalent bond (*11*). The four N-terminal amino acid residues of pVIc interact via hydrogen bonds and van der Waals interactions with residues located in the helical domain of AVP. The first three amino acid residues are in a pocket formed by a turn in AVP that starts at Met141 and extends to Gly152. The bottom of the pocket is in part formed by Gln112−Val114; this is in a region close to the oxyanion hole. Amino acid residues 5′−9′ of pVIc cross between the two domains of AVP, into the β-sheet domain. pVIc forms the sixth strand of the central

I	V	G	L	↓	G	V	Q	S	L	K	R	R	R	C	F
11 ile	12 val	GLY	8 leu		GLY	15 val	4 arg	7 ser	6 leu	11 lys	15 arg	17 arg	12 arg	CYS	13 tyr
5 met	2 ser		4 asp			3 leu	4 lys	3 tyr	5 val	4 thr	2 gln	1 ser	4 tyr		5 phe
2 leu	2 thr		2 val				3 asn	2 asn	2 ser	3 ser	1 leu	1 asn	2 met		
	1 leu		1 asn				3 gln	2 phe	2 gly	1 arg	1 thr		1 gln		
	1 met		1 gln				2 ala	2 thr	1 ala						
			1 ser				2 ser	1 pro	1 ile						
			1 thr					1 val	1 thr						
								1 asn							

FIGURE 3: Conserved amino acid residues of pVIc. The C-terminal sequence of the precursor to protein VI is shown from the AVP consensus cleavage site, for the excision of pVIc, to the C-terminus. Sequences were obtained from database searches of the last 15 amino acid residues of pVI. Identical residues are capitalized, and homologous substitutions are underlined.

β-sheet. The penultimate amino acid of pVIc, Cys10′, is covalently linked via a disulfide bond to Cys104 of AVP.

The C-terminal Phe11′ side chain is locked into a hydrophobic pocket formed in part from side chain interactions between the amino acid residues of pVIc and AVP. These interactions suggest that pVIc acts as a strap that brings the two domains of AVP into the alignment that fosters efficient substrate binding and catalysis. Two amino acids in pVIc, Gly1′ and Cys10′, are strictly conserved (Figure 3). Three other amino acid residues seem to tolerate only one or two substitutions: pVIc2′, mostly Val, sometimes Leu; pVIc8′, all Arg but one Asn and one Ser; and pVIc11′, Phe or Tyr.

K_d for the Binding of pVIc to AVP and K_m and k_{cat} for Substrate Hydrolysis by AVP−pVIc Complexes, in the Absence and Presence of DNA. The K_d for the binding of wild-type pVIc to AVP and the K_m and k_{cat} for substrate hydrolysis by AVP−pVIc complexes, in the absence and presence of DNA, were determined as follows. The K_d for the binding of wild-type pVIc to AVP was measured by incubating different concentrations of pVIc with 20 nM AVP for 5 min in the absence or presence of 1 μM 12-mer ssDNA, adding the substrate (Leu-Arg-Gly-Gly-NH)$_2$-rhodamine (*5*, *12*), and measuring the rate of substrate hydrolysis. Under these conditions, a disulfide bond between pVIc and AVP will not form, as the half-time for that reaction with pVIc-saturated AVP is 29 min (W. J. McGrath and W. F. Mangel, unpublished observation). A plot of the rate of substrate hydrolysis versus pVIc concentration yielded a rectangular hyperbola (data not shown). If one assumes that the rate of substrate hydrolysis at the plateau is the rate from 20 nM AVP saturated with pVIc, then one can calculate $[pVIc]_b$ and $[pVIc]_f$ at any concentration of pVIc, as described in Materials and Methods. The K_d for the binding of pVIc to AVP was 4.4 μM. In the presence of DNA, the K_d dropped 50-fold to 90 nM (Figure 4A). In the absence of DNA, the K_m and k_{cat} values were 2.1 μM and 1.08 s^{-1}, respectively (Table 1). In the presence of DNA, the K_m was 3.8 μM and the k_{cat} was 2.9 s^{-1}.

This binding analysis assumes that one molecule of pVIc binds to one molecule of AVP. To ascertain the stoichiometry, AVP was titrated with pVIc under tight binding conditions, i.e., conditions under which the enzyme concentration is 5-fold greater than the K_d for the binding of AVP to pVIc. At concentrations of pVIc lower than that of AVP, there will be no free pVIc and the rate of substrate hydrolysis will be directly proportional to the concentration of pVIc. At concentrations of pVIc that are greater than that of AVP, AVP will be saturated and the rate of substrate hydrolysis will be independent of pVIc concentration. The data can be characterized by two straight lines whose intersection point

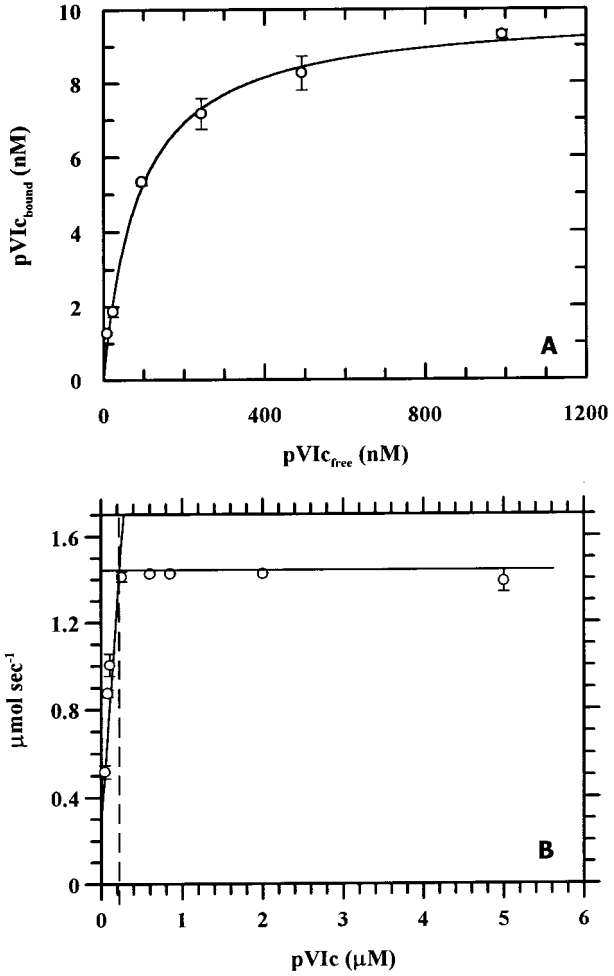

FIGURE 4: Binding and stoichiometry of binding of wild-type pVIc to AVP in the presence of DNA. (A) K_d of wild-type pVIc for AVP, in the presence of DNA. Activity assays were performed using 10 nM AVP and 1 mM 12-mer ssDNA, and $[pVIc]_{bound}$ and $[pVIc]_{free}$ were calculated as described in Materials and Methods. (B) Stoichiometry of binding of pVIc to AVP in the presence of DNA. The assays contained 200 nM AVP, 0.5 mg/mL T7 DNA, and the indicated concentrations of pVIc.

reflects the stoichiometry of binding. Accordingly, 200 nM AVP and 0.5 μg/mL T7 DNA were incubated with increasing concentrations of pVIc, and after 5 min, substrate was added and the rate of substrate hydrolysis determined. The $K_{d(apparent)}$ for the binding of pVIc to AVP in the presence of T7 DNA was 30 nM (data not shown). The data are shown in Figure 4B. Both lines intersect at a point above the abscissa that implies that the stoichiometry of binding of pVIc to AVP is 1:1. This result is also supported by the crystal structure of the AVP−pVIc complex, where one molecule of pVIc is bound to one molecule of AVP (*11*).

Table 1: AVP−pVIc Alanine-Scanning Mutagenesis Results[a]

peptide		K_d (μM)	K_m (μM)	k_{cat} (s^{-1})
GVQSLKRRRCF	DNA (−)	4.43 ± 0.46	2.10 ± 0.76	1.08
	(+)	0.09 ± 0.01	3.83 ± 0.52	2.9
AVQSLKRRRCF	DNA (−)	56.09 ± 6.67	2.94 ± 1.40	1.15
	(+)	0.08 ± 0.01	1.69 ± 0.66	0.75
G**A**QSLKRRRCF	DNA (−)	5.59 ± 0.26	1.79 ± 0.63	0.16
	(+)	0.07 ± 0.02	2.87 ± 0.75	0.89
GV**A**SLKRRRCF	DNA (−)	0.04 ± 0.02	1.86 ± 0.74	0.41
	(+)	0.13 ± 0.04	7.01 ± 1.63	6.79
GVQ**A**LKRRRCF	DNA (−)	4.19 ± 1.97	3.05 ± 0.91	0.52
	(+)	0.10 ± 0.03	1.23 ± 0.45	2.60
GVQS**A**KRRRCF	DNA (−)	0.53 ± 0.09	3.59 ± 0.57	0.61
	(+)	0.03 ± 0.01	3.68 ± 1.46	1.23
GVQSL**A**RRRCF	DNA (−)	5.86 ± 1.17	3.56 ± 0.95	0.50
	(+)	0.42 ± 0.09	1.83 ± 0.76	4.20
GVQSLK**A**RRCF	DNA (−)	0.28 ± 0.05	3.90 ± 0.92	0.50
	(+)	0.10 ± 0.04	1.27 ± 0.39	1.13
GVQSLKR**A**RCF	DNA (−)	3.17 ± 0.01	3.46 ± 1.60	0.84
	(+)	0.21 ± 0.02	4.53 ± 1.85	6.10
GVQSLKRR**A**CF	DNA (−)	0.80 ± 0.23	3.59 ± 1.30	0.56
	(+)	0.14 ± 0.06	2.39 ± 0.44	4.98
GVQSLKRRRC**A**	DNA (−)	28.40 ± 4.05	1.21 ± 0.38	0.21
	(+)	0.24 ± 0.13	1.81 ± 0.54	0.73

[a] Assays were performed in the absence and presence of 1 μM 12-mer DNA. In the presence of 12-mer DNA, the AVP concentration was 20 nM, and in the absence of 12-mer DNA, the AVP concentration was 10 nM. Binding and kinetic constants were calculated as described in Materials and Methods.

Alanine-Scanning Mutagenesis. Alanine-scanning mutagenesis was used to determine the contribution of individual amino acid residues in pVIc to its binding to AVP and to its stimulation of AVP activity. Each amino acid except Cys10′ was individually replaced with an alanine residue. The binding affinities of these 10 mutant pVIcs for AVP were then determined in the presence and absence of 12-mer ssDNA. With the mutant pVIcs bound to AVP, the K_m and k_{cat} for substrate hydrolysis were measured. The results of these assays are summarized in Table 1.

The data from the alanine-scanning mutagenesis experiments indicated that only two side chains contribute significantly to the binding of pVIc to AVP. Interestingly, in the absence of DNA, alanine substitution at five positions led to significantly higher affinity binding. The two amino acid residues most involved in the binding of pVIc to AVP were Gly1′ and Phe11′, which bind 13- and 6-fold weaker than the wild type, respectively. In the absence of DNA, there was a 200-fold variation in K_d over all alanine mutants. In the presence of DNA, this variation is suppressed to only 14-fold. In particular, the binding defect of Gly1′Ala is completely eliminated on DNA binding.

Once bound, several amino acids in pVIc are required for the stimulation of enzyme activity. Both Val2′ and Phe11′ are required for maximal k_{cat} activity in the absence of DNA. Val2′Ala and Phe11′Ala lower k_{cat} 7- and 5-fold, respectively. The variations in K_m were less dramatic than the variations in K_d, 3-fold in the absence of DNA and 6-fold in the presence of DNA. The variation in k_{cat} values in the presence or absence of DNA was ~8-fold.

Major Determinants of Binding in the Absence of DNA. Gly1′ is a major determinant in the binding of pVIc to AVP (Figure 5A). The Gly1′Ala mutant pVIc exhibited a K_d for AVP 13-fold higher than that of wild-type pVIc. In wild-type pVIc, this N-terminal amino acid residue lies in a surface loop of AVP. The amide nitrogen of Gly1′ forms hydrogen bonds with the backbone carbonyls of Met147 and Ile150 and with the side chain carboxyl of Asp142 of AVP (W. J. McGrath and W. F. Mangel, unpublished observation). The carbonyl oxygen atom of Gly1′ forms a hydrogen bond with the nitrogen of Gly152 of AVP. Modeling an Ala in the Gly1′ position results in a steric clash between the introduced methyl group and the carbonyl of Ile150 and the carboxyl group of Asp142. This presumably displaces the first amino acid, disrupting the four hydrogen bonds it normally forms with the protease.

Phe11′ is the other major determinant in the binding of pVIc to AVP (Figure 5B). The Phe11′Ala mutant exhibited a K_d for AVP 6-fold higher than that of wild-type pVIc. In wild-type pVIc, the side chain of Phe11′ is buried in a hydrophobic pocket formed by a salt bridge between pVIc Arg9′ and Glu89 of AVP. In addition, the methylene groups of the side chains of Arg93 and -103, Ile105, and Leu92 of AVP line the pocket. Substitution of Phe11′ with Ala should expose the hydrophobic pocket to solvent, resulting in a lower binding affinity for the pVIc11′ mutant.

Mutants with Improved Binding Affinity. The Gln3′Ala mutation in pVIc resulted in a cofactor whose K_d for AVP

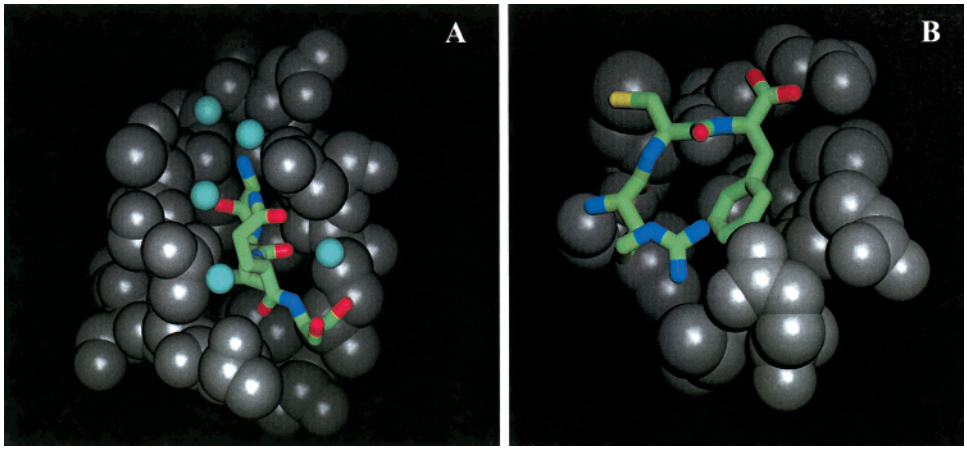

FIGURE 5: Two pVIc binding pockets on AVP. (A) Structure of the binding site on AVP for pVIc residues Gly1′ and Val2′. AVP residues are depicted as CPK spheres. Water molecules are cyan spheres. pVIc residues 1′−3′ are shown in stick format with carbon colored green, nitrogen blue, and oxygen red. (B) Structure of the binding site on AVP for pVIc residues 9′−11′. The same colors used in panel A are used in panel B. The disulfide bond is depicted as a yellow bar.

was 105-fold lower than that of wild-type pVIc. Examination of the crystal structure of an AVP−pVIc complex did not reveal why this mutation should have such a large effect on binding. An alanine at the pVIc3′ position would maintain the backbone hydrogen bond between the carbonyl oxygen and the nitrogen of Thr111 of AVP, but it would lose the side chain interactions with Gln112, Asp142, and the solvent shell. It is possible that the increased affinity of Gln3′Ala is an entropic effect and that immobilization of Gln3′ costs more than is gained from the interactions it makes. Lower K_d values for AVP were also observed with the mutant pVIcs that contained alanine substitutions at residues Leu5′, Arg7′, and Arg9′.

Major Determinants in Stimulating k_{cat}. Clearly, Phe11′ is a major determinant in stimulating the activity of AVP by pVIc. AVP in a complex with the mutant pVIc, Phe11′Ala, exhibited a k_{cat} for substrate hydrolysis that was 5-fold lower than that for the wild-type AVP−pVIc complex. Presumably, disrupting the hydrophobic pocket not only increased the K_d but also decreased the k_{cat}.

The other amino acid residue involved in stimulating the activity of AVP by pVIc was Val2′. The complex of AVP and pVIc mutant Val2′Ala exhibited a catalytic rate constant for substrate hydrolysis 6-fold lower than that with wild-type pVIc. In wild-type pVIc, the side chain of Val2′ lies in a hydrophobic pocket formed by Phe70, Met112, Val114, Met141, and Met147 (Figure 5A). Met112 and Val114 are adjacent to Gln115 that forms part of the oxyanion hole (*9*). It is possible that the lack of an extended hydrophobic side chain at the second position in pVIc causes a repositioning of the side chain of Gln115, thereby altering the oxyanion hole such that it is not optimally positioned for efficient substrate hydrolysis.

Hot Spots in Binding of pVIc to AVP. In protein−protein binding, the free energy of binding at the level of amino acid side chains is typically not distributed evenly across the interface, but is contributed disproportionately by certain amino acids, known as hot spots (*19*). This is true for the binding of pVIc to AVP. A small subset of buried amino acids contributes the majority of binding affinity, as determined by the change in the free energy of binding, $\Delta\Delta G_B$, upon mutation of individual residues to alanine.

The two hot spots in pVIc are Gly1′ and Phe11′. Gly1′ and the side chain of Phe11′ are both buried in the crystal structure. Both residues are largely sequestered from solvent in the complex, with only 20% of the surface area of Gly1′ accessible and 9% of the surface area of the Phe11′ side chain accessible. Although Val2′ is involved in changes in k_{cat}, not K_d, it is also sequestered from bulk solvent, with only 0.01% of its side chain surface area accessible. The solvent occlusion of the hot spots in pVIc is consistent with studies of protein−protein interfaces, showing that solvent exclusion is a necessary condition for tight binding (*19*).

The $\Delta\Delta G_T^*$ upon substitution of an alanine for Gly1′ was 1.57 kcal/mol, and for substitution of an alanine for Phe11′, the $\Delta\Delta G_T^*$ was 1.15 kcal/mol. These are the first and last amino acids of pVIc. The fact that they are hot spots is consistent with the hypothesis that pVIc acts as a strap that brings the two domains of AVP into an alignment more optimal for efficient substrate hydrolysis than in its absence. The amino acid residues most crucial in the binding of pVIc to AVP and in stimulating the activity of AVP are conserved or tolerate only homologous substitution. So far, 18 sequences of pVI have been determined (W. J. McGrath and W. F. Mangel, unpublished observation). The two conserved amino acid residues strictly conserved in pVIc are Gly1′ and Cys10′. Gly1′ is conserved because it is part of the proteinase consensus cleavage sequence, IVGL↓G; cleavage of pVI at this sequence liberates pVIc. Gly1′ is also conserved because no amino acid side chain can fit into the hairpin of AVP that is the binding site for Gly1′. Cys10′ is discussed in another communication. The two other hot spot amino acid residues, Val2′ and Phe11′, tolerate only hydrophobic substitutions.

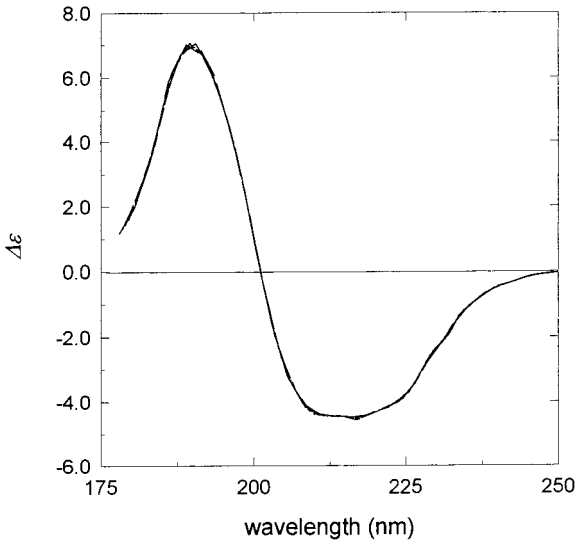

FIGURE 6: Vacuum ultraviolet circular dichroism spectra of AVP and AVP−pVIc, AVP−Ad2 DNA, and AVP−pVIc−Ad2 DNA complexes. Experiments were performed in 10 mM phosphate (pH 7.0). When present, the concentrations of AVP and pVIc were 192 μM, and the concentration of Ad2 DNA was 5.6 nM. Complexes of AVP and pVIc were formed by incubating an equimolar mixture for 10 min at 37 °C. The circular dichroism signals are expressed as the differences in the molar extinction coefficient $\Delta\epsilon$ of the left- and right-handed components (ϵ_L and ϵ_R, respectively) of circularly polarized light as a function of wavelength.

Table 2: Secondary Structures of AVP and AVP−Ad DNA, AVP−pVIc, and AVP−pVIc−Ad2 DNA Complexes Determined by Vacuum Ultraviolet Circular Dichroism

sample	α-helix[a] (%)	β-sheet antiparallel (%)	β-sheet parallel (%)	β-turn (%)	other structure (%)
AVP	39	10	6	15	33
AVP−Ad2 DNA	40	9	8	16	30
AVP−pVIc	40	9	5	13	31
AVP−pVIc−Ad2 DNA	40	11	8	12	29
chymotrypsin[b]	13	25	0	23	38
chymotrypsin[b] (calculated from crystal structure)	10	34	0	20	36

[a] The data in Figure 6 were analyzed by a method that uses inverse CD spectra for each of the five major secondary structures of proteins to predict the fraction of each secondary structure (*21*). [b] From ref *22*.

Effect of DNA on the Binding of pVIc to AVP. The effect of DNA on the binding of pVIc to AVP and on the stimulation of the activity of an AVP−pVIc complex is dramatic. The K_d for the binding of pVIc to AVP bound to DNA decreased 50-fold, to 90 nM, compared to that for the binding of pVIc to AVP in the absence of DNA. In our model

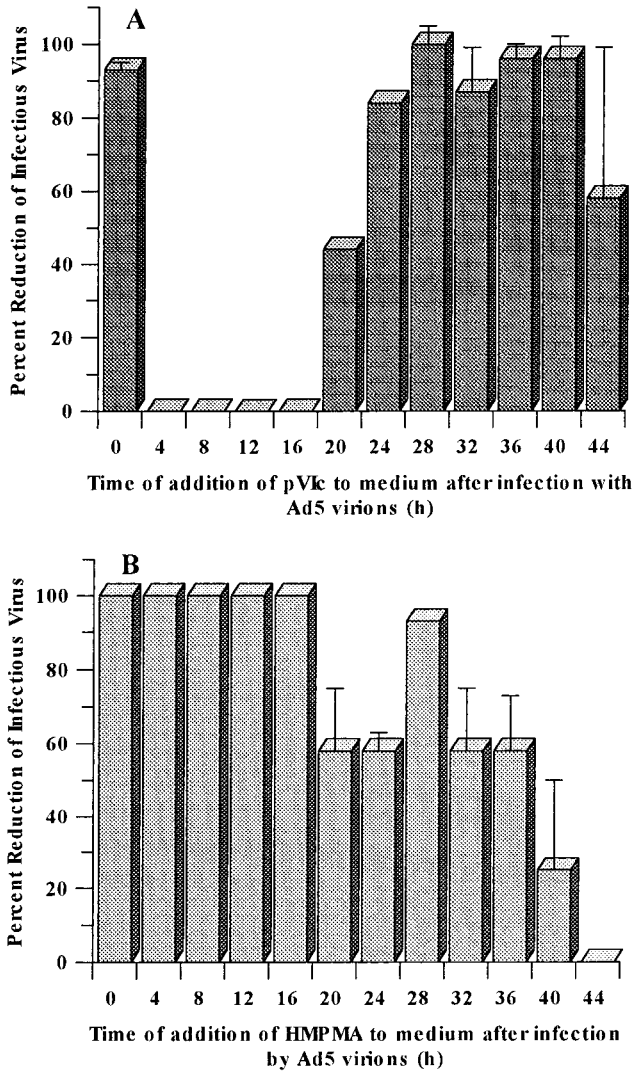

FIGURE 7: pVIc as an antiviral agent. Inhibition of the synthesis of infectious virus by pVIc (A) and by HMPMA (B). Hep-2 cells were seeded in 12-well plates such that upon incubation at 37 °C overnight, 100% confluent monolayers had formed. The cell culture medium was then removed, and to each cell monolayer virus at a multiplicity of infection of 0.001 was added in MEM with 2% FBS. Every 4 h thereafter until 44 h, the virus was removed and either 50 μM pVIc or 140 μM HPMPA, both in MEM with 2% FBS, was added to the cells. The cells were incubated at 37 °C for 48 h. For the zero time point, virus and compound were added simultaneously and remained with the cells for 48 h. Control experiments included cells receiving no compound, no virus, or only medium. The experiments were carried out in duplicate. After a total incubation time of 48 h, the cells were frozen and thawed and the lysates serially diluted using a 10-fold geometric dilution series. Each sample was plated and assayed in triplicate using the CPE assay described by Barnard et al. (*29*). Virus titers were calculated by the Reed-Muensch method described by Sidwell and Huffman (*30*). Virus yield reductions were calculated by subtracting the virus titers at each time point from the virus titer from the wells receiving no treatment. The reduction in virus yield was then expressed as a percentage of untreated, virus-infected controls.

for the regulation of AVP activity, we postulate that AVP bound to the viral DNA cleaves out pVIc from pVI, and the newly released pVIc will then bind to the AVP that cut it out. The greater affinity of pVIc for AVP bound to DNA than for free AVP would ensure the formation of maximally active, ternary complexes (pVIc−AVP−DNA). Additionally, the presence of DNA reversed the effects on K_d of the alanine substitutions. For example, the K_d of Gly1′Ala for AVP was 56 μM. In the presence of DNA, the K_d dropped to 0.08 μM, the same as the K_d for wild-type pVIc binding to AVP. For the alanine mutants of pVIc that exhibited K_d values for binding to AVP lower than that for wild-type pVIc, the presence of DNA altered the K_d values to that of wild-type pVIc. For example, the K_d for AVP with the Gln3′Ala pVIc mutation was 0.04 μM, compared to 4.4 μM with wild-type pVIc. In the presence of DNA, the K_d for the mutant peptide was 0.13 μM, compared to 0.09 μM for wild-type pVIc.

The presence of DNA had little effect on the K_m values but did affect the k_{cat} values. With wild-type pVIc, the presence of 12-mer ssDNA increased the k_{cat} for substrate hydrolysis 3-fold. With the pVIc alanine mutants, e.g., with the Val2′Ala mutant, the k_{cat} was 0.16 s^{-1}. In the presence of DNA, the k_{cat} increased 6-fold to 0.89 s^{-1}, 30% of the wild-type pVIc value.

Importance of the Cysteine Residue of pVIc. The penultimate amino acid in pVIc, Cys10′, is an important amino acid residue (W. J. McGrath and W. F. Mangel, unpublished observation). The K_d for the reversible binding of pVIc to AVP was 4.4 μM. The K_d for the binding of pVIc Cys10′Ala to AVP was difficult to measure and was at least 100-fold higher than that for wild-type pVIc; the K_d decreased at least 60-fold, to 6.93 μM, in the presence of 12-mer ssDNA. Once pVIc Cys10′Ala was bound to an AVP−DNA complex, the macroscopic kinetic constants for substrate hydrolysis were the same as those exhibited by wild-type pVIc. Although the cysteine in pVIc is important in the binding of pVIc to AVP, formation of a disulfide bond between pVIc and AVP was not required for maximal stimulation of enzyme activity by pVIc. At a concentration of pVIc 5 times greater than its K_d for AVP, the time to reach maximal stimulation of enzyme activity by pVIc was 3 min, whereas under identical conditions, the half-time for formation of a disulfide between pVIc and AVP was 29 min.

Changes in Secondary Structure upon Binding of pVIc to AVP. The binding of pVIc to AVP has a profound effect on the rate of substrate hydrolysis in the active site. The pVIc binding site is quite far from the active site. Thus, one might expect that upon binding of pVIc to AVP, a signal would be transduced from the pVIc binding site to the active site that would be mediated by a change in the secondary structure of the enzyme. The vacuum ultraviolet circular dichroism (CD) spectra of AVP and AVP−pVIc, AVP−Ad2 DNA, and AVP−pVIc−Ad2 DNA complexes are shown in Figure 6. There was one positive peak at 190 nm and one broad, negative peak at 215 nm. The spectra were recorded down to 178 nm because while spectra recorded down to 200 nm can be used to determine accurately the amount of α-helix in a protein, they cannot be used to determine other structures such as parallel and antiparallel β-sheets (*20*). The data were analyzed by a method that uses inverse CD spectra for each of the five major secondary structures of proteins (*21*). The results (Table 2) indicated there was considerable α-helix (40%), ∼10% antiparallel β-sheet, ∼7% parallel β-sheet, and ∼14% β-turns. The data indicated that the binding of pVIc and/or Ad2 DNA to AVP did not induce a change in the secondary structure of AVP.

It was surprising that the presence of the cofactors did not alter the secondary structure of AVP. There are several

indications that our results on the secondary structures of the various complexes are reliable. The method of analysis places no constraint on the sum of structures, and the percent of a structure is permitted to be negative. Thus, a sum of structures between 90 and 110% and the absence of a large, negative percent of structure are indicative of a successful analysis (*21*). The sum of structure was 103% for AVP and for AVP−Ad2 DNA complexes, 98% for AVP−pVIc complexes, and 100% for AVP−Ad2 DNA−pVIc complexes. As additional controls, we obtained the CD spectrum of chymotrypsin and analyzed it in an identical way (*22*, *23*). The results compared favorably to the secondary structure of chymotrypsin determined by X-ray crystallography (Table 2). Far-UV spectra, down to 200 nm, have been reported by others of mutant and wild-type AVP (*24*). Their spectra are quite different from ours and indicate that the secondary structure of the AVP−pVIc complex is mainly β-sheet, whereas our data indicate it is mainly α-helix. The 34% α-helical content and the 15% β-strand content of the AVP−pVIc crystal structure (*11*) compare favorably to the values of 40 and 14%, respectively, calculated from the CD spectra in this study.

pVIc as an Antiviral Agent. Our model for the regulation of the adenovirus proteinase activity postulates the enzyme is synthesized in an inactive form because if it were active before virion assembly, it would cleave virion precursor proteins, thereby preventing virion assembly. From this point of view, pVIc could behave as an antiviral agent. To see if pVIc can act as an antiviral agent by prematurely activating the proteinase, we infected Hep-2 cells with Ad5. At the indicated times after infection, the culture medium was replaced with medium containing pVIc or HPMPA, a nucleoside analogue that inhibits viral DNA replication (*25*−*28*). After 48 h, the amount of synthesized infectious virus was titered.

The results indicated that if pVIc was added between 4 and 16 h after infection, there was no reduction in the level of synthesis of infectious virus (Figure 7A). However, if it was added at time zero along with virus or 20 h and beyond, there was a large reduction in the synthesis of infectious virus, 99.8% at 28 h. One interpretation of these data is that they indicate pVIc can enter cells only along with virus and that, when it does, it aborts the synthesis of infectious virus. Inhibition was observed with pVIc added at 20 h and later, because virus is being released and infecting uninfected cells; the multiplicity of infection was 0.001. Our results are quite different from those of Rancourt et al. (*29*). They observed maximum inhibition when pVIc was added to the medium 4, 7, or 10 h after infection. As a control, a similar experiment was carried out with HPMPA (Figure 7B). In this case, there was a 99.8% reduction in the level of synthesis of infectious virus if HPMPA was added between zero and 12 h after infection. At 16 h and beyond, the addition of HPMPA had a lower-magnitude effect on the synthesis of infectious virus. It is doubtful whether pVIc would be a useful antiviral agent clinically. However, these data indicate prematurely inducing enzyme activity is as valid an approach to developing antiviral agents as is inhibiting enzyme activity.

REFERENCES

1. Weber, J. (1976) *J. Virol. 17*, 462−471.
2. Brown, M. T., McGrath, W. J., Toledo, D. L., and Mangel, W. F. (1996) *FEBS Lett. 388*, 233−237.
3. Anderson, C. W., Baum, P. R., and Gesteland, R. F. (1973) *J. Virol. 12*, 241−252.
4. Yeh-Kai, L., Akusjarvi, G., Alestrom, P., Pettersson, U., Tremblay, M., and Weber, J. (1983) *J. Mol. Biol. 167*, 217−222.
5. Mangel, W. F., McGrath, W. J., Toledo, D. L., and Anderson, C. W. (1993) *Nature 361*, 274−275.
6. Anderson, C. W. (1993) *Protein Expression Purif. 4*, 8−15.
7. Webster, A., Hay, R. T., and Kemp, G. (1993) *Cell 72*, 97−104.
8. Webster, A., and Kemp, G. (1993) *J. Gen. Virol. 74*, 1415−1420.
9. Mangel, W. F., Toledo, D. L., Ding, J., Sweet, R. M., and McGrath, W. J. (1997) *Trends Biochem. Sci. 22*, 393−398.
10. Bhatti, A. R., and Weber, J. (1978) *Biochem. Biophys. Res. Commun. 81*, 973−979.
11. Ding, J., McGrath, W. J., Sweet, R. M., and Mangel, W. F. (1996) *EMBO J. 15*, 1778−1783.
12. McGrath, W. J., Abola, A. P., Toledo, D. L., Brown, M. T., and Mangel, W. F. (1996) *Virology 217*, 131−138.
13. Mangel, W. F., Toledo, D. L., Brown, M. T., Martin, J. H., and McGrath, W. J. (1996) *J. Biol. Chem. 271*, 536−543.
14. Gill, S. G., and von Hippel, P. H. (1989) *Anal. Biochem. 182*, 319.
15. Riddles, P. S., Blakeley, R. L., and Zerner, B. (1979) *Anal. Biochem. 94*, 75−81.
16. Hubbard, S. J., and Thornton, J. M. (1993) 'NACCESS' computer program, Department of Biochemistry and Molecular Biology, University College, London.
17. Sutherland, J. C., Desmond, E. J., and Takacs, P. Z. (1980) *Nucl. Instrum. Methods 172*, 195−199.
18. Sutherland, J. C., Keck, P. C., Griffin, K. P., and Takacs, P. Z. (1982) *Nucl. Instrum. Methods 195*, 375−379.
19. Bogan, A. A., and Thorn, K. S. (1998) *J. Mol. Biol. 280*, 1−9.
20. Siegel, J. B., Steinmetz, W. E., and Long, G. L. (1980) *Anal. Biochem. 104*, 160−167.
21. Compton, L. A., and Johnson, W. C., Jr. (1986) *Anal. Biochem. 155*, 155−167.
22. Mangel, W. F., Lin, B., and Ramakrishnan, V. (1990) *Science 248*, 69−73.
23. Mangel, W. F., Lin, H. B., and Ramakrishnan, V. (1990) *J. Biol. Chem. 266*, 9408−9412.
24. Keyvani-Amineh, H., Diouri, M., Guillemette, J. G., and Weber, J. M. (1995) *J. Biol. Chem. 270*, 23250−23253.
25. De Clercq, E. (1991) *Biochem. Pharmacol. 42*, 963−972.
26. Gordon, Y. J., Romanowski, E., Araullo-Cruz, T., Seaberg, L., Erzurum, S., Tolman, R., and De Clercq, E. (1991) *Antiviral Res. 16*, 11−16.
27. Hui, M. B. V., Lien, E. J., and Trousdale, M. D. (1994) *Antiviral Res. 24*, 261−273.
28. Trousdale, M. D., Goldschmidt, P. L., and Nobrega, R. (1994) *Cornea 13*, 435−439.
29. Barnard, D. L., Huffman, J. H., Sidwell, R. W., and Meyerson, L. R. (1993) *Chemotherapy 39*, 203−211.
30. Sidwell, R. W., and Huffman, R. W. (1971) *Appl. Microbiol. 22*, 797−801.
31. McGrath, W. J., Baniecki, M. L., Li, C., McWhirter, S. M., Brown, M. T., Toledo, D. L., and Mangel, W. R. (2001) *Biochemistry*, in press.

BI0109008